Joint Waveform and Clustering Design for Coordinated Multi-point DFRC Systems

Li Chen, *Senior Member, IEEE*, Xiaowei Qin, Yunfei Chen, *Senior Member, IEEE*, and Nan Zhao, *Senior Member, IEEE*

***Abstract*—To improve both sensing and communication performances, this paper proposes a coordinated multi-point (CoMP) transmission design for a dual-functional radar-communication (DFRC) system. In the proposed CoMP-DFRC system, the central processor (CP) coordinates multiple base stations (BSs) to transmit both the communication signal and the dedicated probing signal. The communication performance and the sensing performance are both evaluated by the signal-to-interference-plus-noise ratio (SINR). Given the limited backhaul capacity, we study the waveform and clustering design from both the radar-centric perspective and the communication-centric perspective. Dinkelbach's transform is adopted to handle the single-ratio fractional objective for the radar-centric problem. For the communication-centric problem, we adopt quadratic transform to convexitify the multi-ratio fractional objective. Then, the rank-one constraint of communication beamforming vector is relaxed by semidefinite relaxation (SDR), and the tightness of SDR is further proved to guarantee the optimal waveform design with fixed clustering. For dynamic clustering, equivalent continuous functions are used to represent the non-continuous clustering variables. Successive convex approximation (SCA) is further utilized to convexitify the equivalent functions. Simulation results are provided to verify the effectiveness of all proposed designs.**

***Index Terms*—Beamforming, clustering, coordinated transmission, DFRC, SINR, waveform.**

I. Introduction

Next-generation wireless networks will provide both sensing and communication functionalities to enable various novel applications, e.g., area imaging [1], drone monitoring [2], activity recognition [3], and vehicle platooning [4]. This motivates the research of dual-functional radar-communication (DFRC) by implementing both sensing and communication in the same system. Nevertheless, the realization of DFRC leads to a number of challenges, including information-theoretical limits [5], full-duplex operation [6], multiple access scheme [7], transceiver design [8], resource allocation [9] and so on.

A straightforward DFRC realization is to embed communication signals into radar waveforms. In [10], the authors proposed radar waveform design allowing information delivery to a single or multiple communication directions using the sidelobes of the radar waveform. Designing the radar waveform associated with different constellations, other works have embedded information symbols into the radar pulses based on phase-modulation [11], code shift keying [12] and frequency-hopping code [13]. Using sparse antenna array configurations, the work in [14] embedded communication information into the emission of multiple-input multiple-output (MIMO) radar. The authors in [15] developed a generalized framework for performing information embedding in DFRC systems by accommodating a variety of existing signaling strategies. Although embedding information into radar pulse does not affect the radar performance, its communication rate is limited by the pulse frequency.

To achieve the performance tradeoff between sensing and communication, other works have applied multiple access schemes to the DFRC design. In [16], pseudo-random sequences were adopted to realize both spread-spectrum communication and auto-correlation detection. The authors in [17] and [18] dynamically allocated time slots for radar and communication to achieve their performance tradeoff. A time-division integrated sensing and communication system was proposed in [19] for raw sensing data sharing among connected automated vehicles. The work in [20] proposed a novel multiple access scheme named radar-aware carrier sense multiple access (RA-CSMA) to enable dual functions, which outperformed the above time division multiple access (TDMA) scheme. Based on orthogonal frequency-division multiplexing (OFDM) scheme, the author in [21] studied the DFRC waveform to realize both high data transmission rate and low range sidelobes. Reference [22] studied the use of different multiple access schemes for DFRC systems using signals from multiplexed communications users (CUs).

Beamforming design provides another efficient way for DFRC realization based on the spatial degrees of freedom. The work in [23] proposed a series of transmit beamforming approaches for both separated and shared antenna deployments. In [24], a joint transmit beamforming model was studied for a dual-function MIMO radar and multiuser MIMO communication transmitter. Exploiting the inherent spatial and spectral randomness, a DFRC scheme based on the carrier agile phased array radar was provided by [25]. Regarding the radar targets as potential eavesdroppers, beamforming with artificial noise was designed to enable communication-radar functions in [26]. Integrating reconfigurable intelligent surface (RIS), the beamforming of RIS and radar was jointly optimized

This research was supported by National Key R&D Program of China (Grant No. 2021YFB2900302), and Joint Funds of the National Natural Science Foundation of China (Grant No. U21A20452). (*Corresponding author: Xiaowei Qin*)

L. Chen and X. Qin are with CAS Key Laboratory of Wireless-Optical Communications, University of Science and Technology of China. (e-mail: {chenli87,qinxw}@ustc.edu.cn).

Y. Chen is with the Department of Engineering, University of Durham, Durham, UK, DH1 3LE (e-mail: Yunfei.Chen@durham.ac.uk).

N. Zhao is with the School of Information and Communication Engineering, Dalian University of Technology, Dalian 116024, China. (e-mail: zhaonan@dlut.edu.cn).

to maximize communication performance while maintaining radar detection performance [27]. The work in [28] further studied a RIS-assisted DFRC system, where the base station (BS) simultaneously performs both MIMO radar sensing and multi-user MIMO communication. A space-time coding scheme was developed in [29] for transmit beamforming of DFRC to embed communication information. Fixed covariance for MIMO radar to guarantee the radar performance, signal-to-interference-plus-noise ratio (SINR) balancing problem was solved by multiuser transmit beamforming in [30]. The authors in [31] studied the hybrid beamforming designs for an OFDM-DFRC system.

Most of these existing works on DFRC designs have focused on single-BS scenario. To improve the performance of sensing and communication, coordinated multi-point (CoMP) transmission provides a promising architecture. From the communication perspective, CoMP transmission could exploit inter-cell interference by allowing the user data to be jointly processed by multiple interfering BSs [32]. For example, the work in [33] improved the performance of CoMP communication through joint resource allocation. Considering limited backhaul capacity, the transmission strategy has been studied in [34]. The CoMP architecture was also intended to the networks of unmanned aerial vehicle (UAV) [35], simultaneous wireless information and power transfer (SWIPT) [36] and caching [37] for the benefits of interference mitigation. From the radar perspective, CoMP transsmission could offer improved sensing capability due to enhanced spatial spread as widely separated antennas [38]. Various distributed MIMO radar systems were designed to improve the localization accuracy based on Cramer-Rao bound (CRB) in [39]. With imperfect waveform separation, the target detection problem was modeled and optimized for distributed MIMO radar system in [40]. In presence of time synchronization errors, a closed-form solution to estimate the target position was provided in [41].

However, the above mentioned CoMP designs cannot be applied to the DFRC system, since there exists inherent conflict and tradeoff to improve the performance of radar and communication simultaneously. Also, the complexity of CoMP design for the DFRC system will greatly increase, since the CoMP waveform and clustering should be jointly optimized for both communication and sensing. Recently, an overview of system architecture that enables various types of sensing was first proposed for coordinated mobile networks in [42]. For a multi-UAV DFRC network, the power control problem was studied in [43] to optimize the network utility under the constraint of localization accuracy. The authors in [44] also discussed a CoMP power control problem to minimize the total transmit power while ensuring the SINR of the communication and the CRB of the localization. None of these works has considered the joint waveform and clustering design for the CoMP DFRC system to the best of our knowledge.

Motivated by the above observations, in this paper, the joint waveform and clustering design for CoMP DFRC systems is studied. Specifically, the central processor (CP) coordinates multiple BSs to transmit both the communication signal and the dedicated probing signal for the multi-user communication and the target sensing. We first define the clustering variables of both communication and radar based on the communication beamforming vector and the radar covariance matrix. Then, the signal-to-interference-plus-noise ratio (SINR) is derived for both communication and sensing to evaluate their performance. Given the limited backhaul capacity, we further formulate the waveform and clustering design problems from both the radar-centric perspective and the communication-centric perspective. For fixed clustering, the problems degenerate to the the waveform design problem. Dinkelbach's transform is adopted to simplify the single-ratio fractional objective function in the radar-centric problem. Quadratic transform is adopted to solve the multi-ratio fractional objective function in the communication-centric problem. Further, the rank-one constraint of communication beamforming vector is relaxed by semidefinite relaxation (SDR) with its tightness proved for both problems. For dynamic clustering, equivalent continuous functions are used to express the non-continuous clustering variables of both communication and radar. To convexitify the corresponding problem, successive convex approximation (SCA) is further adopted. The final waveform and clustering designs are provided for both problems with polynomial complexity. The main contributions of this work are summarized as follows.

- The SINR performances of the CoMP DFRC system are derived for both communication and sensing. The corresponding backhaul cost due to the clustering of both communication and radar is modeled. Then, the CoMP waveform and clustering design problem is formulated form both the communication-centric and radar-centric perspectives.
- For the CoMP waveform design, Dinkelbach's transform is used for the radar-centric problem and quadratic transform is used for the communication-centric problem due to the fractional objective functions. SDR is used to relax the rank-one constraint of communication beamforming vector with the tightness proved. Thus, the optimal waveform design can be achieved with fixed clustering.
- For the CoMP clustering design, equivalent continuous functions are adopted to express the non-continuous variables of both the communication clustering and the radar clustering. In order to further convexitify the equivalent constraints, we adopt SCA to approximate the corresponding non-convex constraints. A sub-optimal clustering solution can be given based on the algorithms with polynomial complexity.

The remainder of the paper is organized as follows. Section II presents the system model. Section III gives the performance analysis of the CoMP DFRC system and formulates the CoMP design problem from both radar-centric and communication-centric points of view. The corresponding solutions of the waveform and clustering designs are provided in Section IV. Simulation results are provided in Section V, followed by concluding remarks in Section VI.

Notation: We use boldface lowercase letter to denote column vectors, and boldface uppercase letters to denote matrices. Superscripts $(\cdot)^H$ and $(\cdot)^T$ stand for Hermitian transpose and transpose, respectively. $\mathrm{tr}(\cdot)$, $\mathrm{diag}(\cdot)$, and $\mathrm{rank}(\cdot)$ represent the

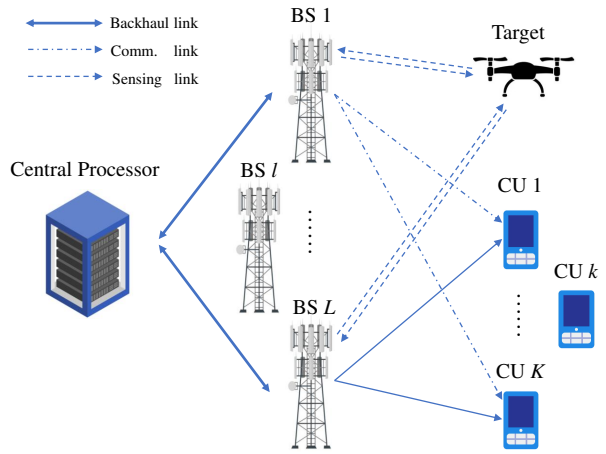

Figure 1. CoMP transmission for a DFRC system with a CP, L multi-antenna BSs, K single-antenna CUs and a point-like target.

trace operation, the vector formed by the diagonal elements and the rank operator, respectively. $\det(\cdot)$ is the determinant of a matrix. $\mathcal{C}^{m\times n}$ is the set of complex-valued $m \times n$ matrices. $\mathbf{C} \succeq 0$ denotes the matrix $\mathbf{C}$ is positive semi-definite. $x \sim \mathcal{CN}(a,b)$ means that x obeys a complex Gaussian distribution with mean a and covariance b. $\mathrm{E}(\cdot)$ denotes the statistical expectation. $\|\mathbf{x}\|$ denotes the Euclidean norm of a complex vector $\mathbf{x}$.

II. System Model

As illustrated in Fig.1, consider the CoMP transmission for a DFRC system composed of a CP, L dual-functional BSs indexed by $l \in \{1,\cdots,L\}$, K CUs indexed by $k \in \{1,\cdots,K\}$, and a point-like target. Each BS is equipped with N transmit antennas and M receive antennas. The CP coordinates multiple BSs to serve the CUs and detect the target simultaneously.

Given the coordinated transmit signal of the BSs, i.e., $\mathbf{x} \in \mathcal{C}^{NL\times 1}$, the received signal at the CU k is

$$y_k = \mathbf{h}_k^H \mathbf{x} + z_k, \tag{1}$$

where $\mathbf{h}_k \in \mathcal{C}^{NL\times 1}$ is the channel between all BSs and the CU k, $z_k \sim \mathcal{CN}(0,\sigma_k^2)$ is the additive white Gaussian noise (AWGN) at the CU k, and the time instance is omitted for conciseness.

The dual-functional BSs also work as a colocated monostatic MIMO radar. Assuming I signal-dependent interferences indexed by $i \in \{1,\cdots,I\}$, the received signal at the BSs aligned to the target delay can be expressed as

$$\mathbf{y}_0 = \alpha_0 \mathbf{A}(\theta_0)\mathbf{x} + \sum_{i=1}^{I} \alpha_i \mathbf{A}(\theta_i)\mathbf{x} + \mathbf{z}_0, \tag{2}$$

where $\alpha_j \mathbf{A}(\theta_j)$ is the response matrix of a target ($j=0$) or an interference ($j=1,\cdots,I$) with α_j being the radar cross section (RCS) and $\theta_j = \{\theta_{j,1},\cdots,\theta_{j,L}\}$ being the azimuth angle of the BSs,

$$\begin{aligned}\mathbf{A}(\theta_j) = &[1;\cdots;e^{-j2\pi(N-1)\Delta_t \sin\theta_{j,1}};\cdots;1;\cdots;e^{-j2\pi(N-1)\Delta_t \sin\theta_{j,L}}]^T \\ &[1;\cdots;e^{-j2\pi(M-1)\Delta_r \sin\theta_{j,1}};\cdots;1;\cdots;e^{-j2\pi(M-1)\Delta_r \sin\theta_{j,L}}]\end{aligned} \tag{3}$$

with Δ_t and Δ_r being the spacing between the adjacent transmit and receive antennas normalized by the wavelength, and $\mathbf{z}_0 \in \mathcal{C}^{N_r\times 1}$ is the AWGN at the radar receiver with each element subjects to $\mathcal{CN}(0,\sigma_0^2)$. This assumes the presence of target.

For dual-functional realization, the coordinated transmit signal of all BSs in (1) and (2) is

$$\mathbf{x} = \sum_{k=1}^{K} \mathbf{b}_k d_k + \mathbf{v}, \tag{4}$$

where $\mathbf{b}_k \in \mathcal{C}^{NL\times 1}$ is the beamforming vector of all BSs to the CU k, d_k is the data symbol of the CU k satisfying $\mathcal{CN}(0,\sigma_k^2)$ without loss of generality, and $\mathbf{v} \in \mathcal{C}^{NL\times 1}$ is the dedicated probing signal of all BSs for the target sensing. The dedicated probing signal is assumed to be uncorrelated with the data signal. Thus, the covariance matrix of the transmit signal can be calculated as

$$\mathbf{C} = \sum_{k=1}^{K} \mathbf{B}_k + \mathbf{V}, \tag{5}$$

where $\mathbf{B}_k = \mathbf{b}_k \mathbf{b}_k^H$ is the covariance matrix of the communication signal for the CU k satisfying $\mathrm{rank}(\mathbf{B}_k) = 1$, and $\mathbf{V}$ is the covariance matrix of the dedicated probing signal. This assumes $\mathrm{E}[|d_k|^2] = 1$ without loss of generality.

The type of CoMP discussed in this paper is joint transmission (JT). Specifically, for the JT CoMP, multiple points transmit simultaneously in a coherent manner. And the coordinated transmission of the DFRC system is designed at the CP. Using the channel state information (CSI) of the communication and the response matrix of the sensing, the CP designs the clustering policy for both the radar and the communication. Then, it broadcasts the designed policy and the data symbols to the BSs via backhaul links.

In order to evaluate the corresponding backhaul cost, the beamforming vector of all BSs to the CU k can be further decomposed as

$$\mathbf{b}_k = \left[\mathbf{b}_{k,1}^H \mathbf{b}_{k,2}^H \cdots \mathbf{b}_{k,L}^H\right]^H, \tag{6}$$

where $\mathbf{b}_{k,l} \in \mathcal{C}^{N\times 1}$ is the beamforming vector of the BS l to the CU k. Also, the dedicated probing signal of the BSs can be further expressed as

$$\mathbf{v} = \left[\mathbf{v}_1^H \mathbf{v}_2^H \cdots \mathbf{v}_L^H\right]^H \tag{7}$$

where $\mathbf{v}_l \in \mathcal{C}^{N\times 1}$ is the dedicated probing signal of the BS l.

Unlike existing CoMP systems, both the communication clustering and the radar clustering should be considered in the DFRC system. We define the communication clustering variables and the radar clustering variables as

$$s_{k,l} = \begin{cases} 1, & \|\mathbf{b}_{k,l}\|^2 > 0 \\ 0, & \|\mathbf{b}_{k,l}\|^2 = 0 \end{cases}, \forall k,l \tag{8}$$

and

$$c_l = \begin{cases} 1, & \|\mathbf{v}_l\|^2 > 0 \\ 0, & \|\mathbf{v}_l\|^2 = 0 \end{cases}, \forall l \tag{9}$$

respectively, where $s_{k,l} = 1$ indicates that the l-th BS belongs to the communication cluster serving the k-th CU, and $s_{k,l} = 0$ otherwise, $v_l = 1$ indicates that the l-th BS belongs to the radar cluster detecting the target, and $v_l = 0$ otherwise.

Note that if a BS transmits the communication signal and the dedicated radar signal simultaneously, it belongs to both clusters at the same time. If a BS only transmits the communication signal or the dedicated radar signal, it belongs to the communication cluster or the radar cluster. Specifically, the coordinated transmit signal of BS l can be given by $\mathbf{x}_l = \sum_{k=1}^{K} \mathbf{b}_{k,l} d_k + \mathbf{v}_l$. If the communication clustering variables $s_{k,l} = 1$, i.e., $\|\mathbf{b}_{k,l}\|^2 > 0$, the BS l belongs to the communication cluster. And if the radar clustering variables $v_l = 1$, i.e., $\|\mathbf{v}_l\|^2 > 0$, the BS l belongs to the radar cluster.

According to (6) and (7), the transmit power of the BS l can be calculated by

$$\begin{aligned} p_l &= \sum_{k=1}^{K} \|\mathbf{b}_{k,l}\|^2 + \|\mathbf{v}_l\|^2 \\ &= \sum_{k=1}^{K} \mathrm{tr}\left(\mathbf{J}_l \mathbf{B}_k\right) + \mathrm{tr}\left(\mathbf{J}_l \mathbf{V}\right) \\ &= \mathrm{tr}\left(\mathbf{J}_l \mathbf{C}\right) \end{aligned} \tag{10}$$

where $\mathbf{J}_l$ is a selection matrix of the BS l given by $\mathbf{J}_l = \mathrm{diag}\left\{\mathbf{0}^H_{(l-1)M}, \mathbf{I}_M, \mathbf{0}^H_{(L-l)M}\right\}$.

To reduce the overhead, smaller size cooperation clusters are required where coordination only takes place within the cluster. And the total backhaul cost of the whole system can be derived as

$$b = \sum_{k=1}^{K} \sum_{l=1}^{L} s_{k,l} \beta_{k,l} + \sum_{l=1}^{L} c_l \beta_l{}', \tag{11}$$

where $\beta_{k,l}$ is the communication backhaul cost of the BS l serving the CU k, and $\beta_l{}'$ is the radar backhaul cost of the BS l detecting the target. The communication backhaul delivers the CSI of the communication, the data symbols and the designed beamforming vector, while the radar backhaul delivers the response matrix of the radar and the designed dedicated probing signal. Thus, the backhaul costs of the communication and the radar are generally different.

III. Performance Analysis and Problem Formulation

In this section, we analyze the performance of the CoMP transmission for the DFRC system. In order to jointly design the transmit waveform and the clustering, two optimization problems are formulated from the radar-centric perspective and the communication-centric perspective, respectively.

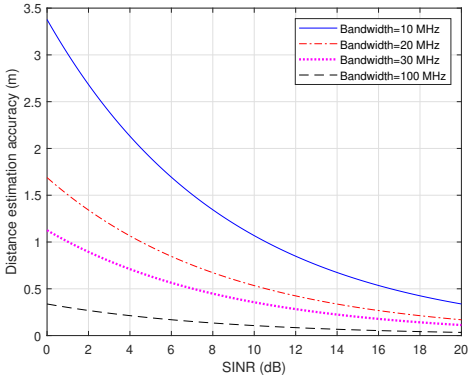

Figure 2. The illustration of the location performance of the target versus the sensing SINR of the target.

A. Performance Analysis

In this work, we adopt SINR as the performance metric of the DFRC system for both communication and sensing. For the communication, the received SINR at the CUs determines the communication rate. It is assumed that we consider a quasi-static channel for both the communication and the radar, where the CSI and the response matrix are constant during the design.

Given the coordinated transmit signal in (4), the received signal at the CU k in (1) can be rewritten as

$$y_k = \mathbf{h}_k^H \mathbf{b}_k d_k + \mathbf{h}_k^H \sum_{i=1, i\neq k}^{K} \mathbf{b}_i d_i + \mathbf{h}_k^H \mathbf{v} + z_k. \tag{12}$$

Thus, the received SINR of the CU k can be calculated by

$$\begin{aligned} \gamma_k &= \frac{\left|\mathbf{h}_k^H \mathbf{b}_k\right|^2}{\sum\limits_{i=1, i\neq k}^{K} \left|\mathbf{h}_k^H \mathbf{b}_i\right|^2 + \left|\mathbf{h}_k^H \mathbf{v}\right|^2 + \sigma_k^2} \\ &= \frac{\mathrm{tr}\left(\mathbf{H}_k \mathbf{B}_k\right)}{\sum\limits_{i=1, i\neq k}^{K} \mathrm{tr}\left(\mathbf{H}_k \mathbf{B}_i\right) + \mathrm{tr}\left(\mathbf{H}_k \mathbf{V}\right) + \sigma_k^2}, \\ &= \frac{\mathrm{tr}\left(\mathbf{H}_k \mathbf{B}_k\right)}{\mathrm{tr}\left(\mathbf{H}_k \mathbf{C}\right) - \mathrm{tr}\left(\mathbf{H}_k \mathbf{B}_k\right) + \sigma_k^2}. \end{aligned} \tag{13}$$

where $\mathbf{H}_k = \mathbf{h}_k \mathbf{h}_k^H$, and the covariance matrices $\{\mathbf{B}_k\}$, $\mathbf{V}$ are defined in (5).

For the sensing, the received SINR for the target sensing determines both the detection performance and the localization performance of the target. For example, the distance estimation accuracy versus different SINR for the target sensing is shown in Fig. 2 with different effective signal bandwidth [45].

Using the receive beamforming vector $\mathbf{w} \in \mathcal{C}^{ML}$, the received signal for the probing target in (2) can be further expressed as

$$r_0 = \alpha_0 \mathbf{w}^H \mathbf{A}\left(\theta_0\right) \mathbf{x} + \mathbf{w}^H \sum_{i=1}^{I} \alpha_i \mathbf{A}\left(\theta_i\right) \mathbf{x} + \mathbf{w}^H \mathbf{z}_0. \tag{14}$$

Thus, the received SINR for the target sensing can be calculated as

$$\gamma_0 = \frac{\mathrm{E}\left[\left|\alpha_0 \mathbf{w}^H \mathbf{A}\left(\theta_0\right)\mathbf{x}\right|^2\right]}{\mathrm{E}\left[\left|\mathbf{w}^H \sum\limits_{i=1}^{I} \alpha_i \mathbf{A}\left(\theta_i\right)\mathbf{x}\right|^2\right] + \sigma_0^2} = \frac{\left|\alpha_0\right|^2 \mathrm{tr}\left(\mathbf{R}_0\mathbf{C}\right)}{\sum\limits_{i=1}^{I}\left|\alpha_i\right|^2 \mathrm{tr}\left(\mathbf{R}_i\mathbf{C}\right) + \sigma_0^2}, \tag{15}$$

where $\mathbf{w}^H\mathbf{w} = 1$ without loss of generality, and $\mathbf{R}_i$ is the constant matrix with fixed receive beamforming vector, which is defined by

$$\mathbf{R}_j = \mathbf{A}^H\left(\theta_j\right)\mathbf{w}\mathbf{w}^H\mathbf{A}\left(\theta_j\right), \forall j = 0, 1, \cdots, I. \tag{16}$$

The optimal $\mathbf{w}$ to maximize the SINR for the target sensing can be derived by solving the equivalent minimum variance distortionless response (MVDR) problem in [46]. Thus, we focus on the design with fixed $\mathbf{w}$ in the following discussion.

B. Problem Formulation

The joint waveform and clustering designs for coordinated multi-point DFRC systems have two distinct goals. One is to maximize the communication performance, i.e., the minimum SINR of all CUs. The other is to maximize the radar performance, i.e., the sensing SINR of the target. Thus, two problems are formulated in this work. First, we consider a radar-centric problem, which aims to maximize the received SINR for the target sensing subject to the constraints of each CU's SINR. The CoMP waveform and clustering design is expected to optimize the sensing performance with fixed communication performance guaranteed. The corresponding problem can be formulated by

$$\begin{aligned}
(\mathrm{P1}) \quad & \max_{\substack{\{\mathbf{B}_k\},\mathbf{C}\\ \{s_{k,l}\},\{c_l\}}} \quad \frac{\left|\alpha_0\right|^2 \mathrm{tr}\left(\mathbf{R}_0\mathbf{C}\right)}{\sum\limits_{i=1}^{I}\left|\alpha_i\right|^2 \mathrm{tr}\left(\mathbf{R}_i\mathbf{C}\right) + \sigma_0^2} \\
\text{s.t.} \quad & \mathrm{C1}: \quad \frac{\mathrm{tr}\left(\mathbf{H}_k\mathbf{B}_k\right)}{\mathrm{tr}\left(\mathbf{H}_k\mathbf{C}\right) - \mathrm{tr}\left(\mathbf{H}_k\mathbf{B}_k\right) + \sigma_k^2} \geq \Gamma_k, \forall k \\
& \mathrm{C2}: \quad \mathrm{tr}\left(\mathbf{J}_l\mathbf{C}\right) \leq P_l, \forall l \\
& \mathrm{C3}: \quad \sum_{k=1}^{K}\sum_{l=1}^{L} s_{k,l}\beta_{k,l} + \sum_{l=1}^{L} c_l {\beta_l}' \leq B \\
& \mathrm{C4}: \quad \mathbf{C} \succeq 0, \mathbf{B}_k \succeq 0, \forall k \\
& \mathrm{C5}: \quad \mathbf{C} - \sum_{k=1}^{K}\mathbf{B}_k \succeq 0 \\
& \mathrm{C6}: \quad \mathrm{rank}\left(\mathbf{B}_k\right) = 1, \forall k \\
& \mathrm{C7}: \quad s_{k,l} \in \{0,1\}, c_l \in \{0,1\}, \forall k, l \\
& \mathrm{C8}: \quad \mathrm{tr}\left(\mathbf{J}_l\mathbf{B}_k\right) \leq s_{k,l}P_l, \forall k, l \\
& \mathrm{C9}: \quad \mathrm{tr}\left[\mathbf{J}_l\left(\mathbf{C} - \sum_{k=1}^{K}\mathbf{B}_k\right)\right] \leq v_l P_l, \forall l
\end{aligned} \tag{17}$$

where Γ_k in the constraint (C1) is the SINR threshold of the CU k, P_l in the constraint (C2) is the maximum transmit power of the BS l, B in the constraint (C3) is the maximum backhaul capacity, the constraints (C4) and (C5) guarantee the positive semidefinite of the covariance matrices of the communication signal and the dedicated probing signal, the constraint (C6) is the rank-one constraint of the communication beamforming vector, the constraint (C7) denotes the non-continuous clustering variables of both communication and radar, the constraint (C8) restricts the transmit power of the BS l for the communication signal when the BS l is not in the communication cluster, and the constraint (C9) imposes a similar restriction on the transmit power of the BS l when the BS l is not in the radar cluster.

Also, consider a communication-centric problem, which aims to maximize the minimum SINR of the CUs with constraints on the target sensing. The CoMP waveform and clustering design is expected to optimize the communication performance with the constant sensing performance guaranteed. The corresponding problem can be formulated by

$$\begin{aligned}
(\mathrm{P2}) \quad & \max_{\substack{\{\mathbf{B}_k\},\mathbf{C},\\ \{s_{k,l}\},\{c_l\}}} \quad \min_k \quad \frac{\mathrm{tr}\left(\mathbf{H}_k\mathbf{B}_k\right)}{\mathrm{tr}\left(\mathbf{H}_k\mathbf{C}\right) - \mathrm{tr}\left(\mathbf{H}_k\mathbf{B}_k\right) + \sigma_k^2} \\
\text{s.t.} \quad & \mathrm{C0}: \quad \frac{\left|\alpha_0\right|^2 \mathrm{tr}\left(\mathbf{R}\left(\theta_0\right)\mathbf{C}\right)}{\sum\limits_{i=1}^{I}\left|\alpha_i\right|^2 \mathrm{tr}\left(\mathbf{R}\left(\theta_i\right)\mathbf{C}\right) + \sigma_0^2} \geq \Gamma_0 \\
& \mathrm{C2}: \quad \mathrm{tr}\left(\mathbf{J}_l\mathbf{C}\right) \leq P_l, \forall l \\
& \mathrm{C3}: \quad \sum_{k=1}^{K}\sum_{l=1}^{L} s_{k,l}\beta_{k,l} + \sum_{l=1}^{L} c_l {\beta_l}' \leq B \\
& \mathrm{C4}: \quad \mathbf{C} \succeq 0, \mathbf{B}_k \succeq 0, \forall k \\
& \mathrm{C5}: \quad \mathbf{C} - \sum_{k=1}^{K}\mathbf{B}_k \succeq 0, \\
& \mathrm{C6}: \quad \mathrm{rank}\left(\mathbf{B}_k\right) = 1, \forall k \\
& \mathrm{C7}: \quad s_{k,l} \in \{0,1\}, c_l \in \{0,1\}, \forall k, l \\
& \mathrm{C8}: \quad \mathrm{tr}\left(\mathbf{J}_l\mathbf{B}_k\right) \leq s_{k,l}P_l, \forall k, l \\
& \mathrm{C9}: \quad \mathrm{tr}\left[\mathbf{J}_l\left(\mathbf{C} - \sum_{k=1}^{K}\mathbf{B}_k\right)\right] \leq v_l P_l, \forall l
\end{aligned} \tag{18}$$

where Γ_0 in the constraint (C0) is the received SINR threshold for the target sensing, and the other constraints are the same as the constraints (C2-C9) of the problem (P1).

Theoretically, there exists inherent conflict and tradeoffs for the joint design to optimize the multiple objectives simultaneously. And the optimal performance tradeoff between the MIMO radar and the MU-MIMO communication can be characterized by the Pareto boundary of the achievable performance region. Considering the practical implementation, the radar-centric joint waveform and clustering designs focus to improve the radar performance as much as possible. Thus, it is suitable to the scenarios where radar functionality

needs to be prioritized, such as unmanned positioning, lane marking detection, obstacle detection, and so on. Further, the communication-centric joint waveform and clustering designs focus to improve the communication performance as much as possible. Thus, it is suitable to the scenarios where communication functionality needs to be prioritized, such as V2V communication, V2I communication, and so on.

IV. Proposed Solutions for CoMP DFRC

In this section, we will solve the radar-centric problem (P1) and the communication-centric problem (P2) to provide optimal CoMP waveform and clustering designs for the DFRC system. And we jointly design the transmit waveform and the cluster association based on the same performance metric. Specifically, from the radar-centric viewpoint, the joint design is optimized to maximize the received SINR for the target sensing subject to the constraints of each CU's SINR. And from the communication-centric viewpoint, the joint design is optimized to optimize the communication performance with the constant sensing performance guaranteed.

A. Radar-centric Problem

The radar-centric problem (P1) in (17) is non-convex for the following reasons. First, the objective function of the problem (P1) is a fractional function. Also, the rank-one constraint (C6) of the beamforming vector is non-convex. Finally, the clustering variables of both communication and radar are non-continuous. In order to avoid brute-force searching, we propose the following two-step design.

1) Waveform optimization: We first consider the radar-centric problem with fixed clustering. Thus, the constraints (C3) and (C7) of clustering variables can be relaxed. The original problem (P1) can be simplified as the waveform optimization problem, i.e.,

$$\begin{aligned}(\text{P1.1}) \quad \max_{\{\mathbf{B}_k\},\mathbf{C}} \quad & \frac{|\alpha_0|^2 \text{tr}\left(\mathbf{R}_0\mathbf{C}\right)}{\sum\limits_{i=1}^{I}|\alpha_i|^2 \text{tr}\left(\mathbf{R}_i\mathbf{C}\right)+\sigma_0^2}, \\ \text{s.t.} \quad & \text{C1, C2, C4, C5,C6, C8, C9}\end{aligned} \tag{19}$$

which optimizes the beamforming vector of the communication signal and the covariance matrix of the dedicated probing signal.

The waveform problem (P1.1) is still non-convex due to the fractional objective function and the non-convex rank-one constraint (C6). For the single-ratio objective function, Dinkelbach's transform can be introduced, where the waveform optimization problem (P1.1) can be converted to the following problem.

$$\begin{aligned}(\text{P1.2}) \quad \max_{\{\mathbf{B}_k\},\mathbf{C}} \quad & |\alpha_0|^2 \text{tr}\left(\mathbf{R}_0\mathbf{C}\right) - \tau \sum_{i=1}^{I}|\alpha_i|^2 \text{tr}\left(\mathbf{R}_i\mathbf{C}\right) - \tau\sigma_0^2, \\ \text{s.t.} \quad & \text{C1, C2, C4, C5, C6, C8, C9}\end{aligned} \tag{20}$$

where τ is an auxiliary variable. Then, we have the following lemma of Dinkelbach's transform.

Lemma 1. (**Optimality of Dinkelbach's transform**) By alternatively optimizing the problem (P1.2) with fixed τ and updating the auxiliary variable τ as

$$\tau = \frac{|\alpha_0|^2 \text{tr}\left(\mathbf{R}_0\mathbf{C}\right)}{\sum\limits_{i=1}^{I}|\alpha_i|^2 \text{tr}\left(\mathbf{R}_i\mathbf{C}\right)+\sigma_0^2}, \tag{21}$$

the optimal solution to the problem (P1.2) converges to the global optimal solution to the problem (P1.1).

Proof. Because τ is non-decreasing after each iteration, the convergence can be guaranteed by alternatively updating τ according to (21) and solving the problem (P1.2). Further, because the problem (P1.1) is a concave-convex fractional problem, the optimal solution to the problem (P1.2) by alternatively updating τ converges to the global optimal solution to the problem (P1.1) according to [47, Proposition 3.1]. □

Note that the problem (P1.2) is still non-convex due to the rank-one constraint (C6). Thus, SDR can be adopted to relax this constraint, and the problem (P1.2) can be relaxed as

$$\begin{aligned}(\text{P1.3}) \quad \max_{\{\mathbf{B}_k\},\mathbf{C}} \quad & |\alpha_0|^2 \text{tr}\left(\mathbf{R}_0\mathbf{C}\right) - \tau \sum_{i=1}^{I}|\alpha_i|^2 \text{tr}\left(\mathbf{R}_i\mathbf{C}\right) - \tau\sigma_0^2, \\ \text{s.t.} \quad & \text{C1, C2, C4, C5, C8, C9}\end{aligned} \tag{22}$$

which is a semidefinite programming (SDP) problem and can be solved using a generic SDP solver.

Generally, SDR will not generate a rank-one solution. Thus, approximating methods such as randomization and scaling [48] should be applied to generate a sub-optimal rank-one solution. The tightness of SDR for the problem (P1.2) can be guaranteed according to the following lemma.

Lemma 2. (**Tightness of SDR**) After applying SDR to the problem (P1.2), the problem (P1.3) is convex and the corresponding global optimal solution can be denoted by $\hat{\mathbf{C}}, \{\tilde{\mathbf{B}}_k\}$. Although $\{\tilde{\mathbf{B}}_k\}$ may not satisfy rank-one constraint, we can obtain a rank-one optimal solution for the problem (P1.3) based on $\{\tilde{\mathbf{B}}_k\}$ as

$$\hat{\mathbf{B}}_k = \frac{\tilde{\mathbf{B}}_k\mathbf{h}_k\mathbf{h}_k^H\tilde{\mathbf{B}}_k^H}{\mathbf{h}_k^H\tilde{\mathbf{B}}_k\mathbf{h}_k}, \forall k \tag{23}$$

satisfying $\text{rank}(\hat{\mathbf{B}}_k) = 1, \forall k$.

Proof. The tightness of SDR for the problem (P1.2) can be proved following [24]. Given the optimal solution $\hat{\mathbf{C}}$ and $\{\tilde{\mathbf{B}}_k\}$ of the problem (P1.3), it can be verified that $\{\hat{\mathbf{B}}_k\}$ in (23) is also a global optimal solution to the problem (P1.3). Since the covariance matrix of the transmit signal $\mathbf{C}$ does not have rank constraint, and the objective function of the problem (P1.3) is only determined by $\mathbf{C}$, we only need to prove that the covariance matrix of the communication signal $\{\hat{\mathbf{B}}_k\}$ in (23) satisfies all constraints of the problem (P1.3). Specifically, it can be verified that

$$\frac{\mathrm{tr}\left(\mathbf{H}_k\hat{\mathbf{B}}_k\right)}{\mathrm{tr}\left(\mathbf{H}_k\hat{\mathbf{C}}\right)-\mathrm{tr}\left(\mathbf{H}_k\hat{\mathbf{B}}_k\right)+\sigma_k^2}\geq\Gamma_k, \tag{24}$$

when $\hat{\mathbf{B}}_k \succeq 0$, $\mathrm{tr}\left(\mathbf{J}_l\hat{\mathbf{B}}_k\right)\leq s_{k,l}P_l$, $\mathrm{tr}[\mathbf{J}_l(\hat{\mathbf{C}}-\sum_{k=1}^K\hat{\mathbf{B}}_k)]\leq v_lP_l\ \forall k,l$. This shows that $\{\hat{\mathbf{B}}_k\}$ in (23) is also an optimal solution to the problem (P1.3), which completes the proof. We refer readers to [24, Theorem 1] for a detailed proof. □

Finally, the waveform optimization problem with fixed clustering, i.e., the problem (P1.1), can be solved according to the following proposition.

Proposition 1. (Solution to waveform optimization) With fixed clustering, the waveform optimization problem (P1.1) can be solved by optimizing the convex SDR problem (P1.3) and updating the auxiliary variable according to (21).

Proof. According to Lemma 2, we can always obtain a rank-one optimal solution after SDR for the problem (P1.3), which is also the optimal solution to the problem (P1.2). Further, according to Lemma 1, the optimal solution to the problem (P1.2) converges to the global optimal solution of the problem (P1.1) by alternatively updating τ according to (21). It completes the proof. □

2) Clustering optimization: Next, we consider the radar-centric problem with dynamic clustering. Then, the waveform design problem (P1.3) can be reformulated with dynamic clustering variables as

$$\begin{aligned}(\mathrm{P1.4})\quad \max_{\substack{\{\mathbf{B}_k\},\mathbf{C},\\ \{s_{k,l}\},\{c_l\}}}\ & |\alpha_0|^2\mathrm{tr}\left(\mathbf{R}_0\mathbf{C}\right)-\tau\sum_{i=1}^I|\alpha_i|^2\mathrm{tr}\left(\mathbf{R}_i\mathbf{C}\right)-\tau\sigma_0^2\\ \text{s.t.}\ & \mathrm{C1}\sim\mathrm{C5},\mathrm{C7}\sim\mathrm{C9}\end{aligned} \tag{25}$$

with the constraints of clustering variables (C3) and (C7) added. The problem (P1.4) becomes non-convex due to the non-continuous clustering variables, i.e., the constraint (C7). Thus, we first adopt equivalent continuous functions to express the non-continuous variables [49]. For the communication clustering variables $s_{k,l}\in\{0,1\},\forall k,l$, they have the following equivalent expression.

$$0\leq s_{k,l}\leq 1, \tag{26}$$

and

$$\sum_{l=1}^L\sum_{k=1}^K s_{k,l}-\sum_{l=1}^L\sum_{k=1}^K s_{k,l}^2\leq 0. \tag{27}$$

For the radar clustering variables $v_l\in\{0,1\},\forall l$, they can be expressed by

$$0\leq v_l\leq 1, \tag{28}$$

and

$$\sum_{l=1}^L v_l-\sum_{l=1}^L v_l^2\leq 0. \tag{29}$$

According to (26-29), by rewriting the constraint (C7), the problem (P1.4) becomes

$$\begin{aligned}(\mathrm{P1.5})\quad \max_{\substack{\{\mathbf{B}_k\},\mathbf{C},\\ \{s_{k,l}\},\{c_l\}}}\ & |\alpha_0|^2\mathrm{tr}\left(\mathbf{R}_0\mathbf{C}\right)-\tau\sum_{i=1}^I|\alpha_i|^2\mathrm{tr}\left(\mathbf{R}_i\mathbf{C}\right)-\tau\sigma_0^2\\ \text{s.t.}\ & \mathrm{C1}\sim\mathrm{C5},\mathrm{C8},\mathrm{C9}\\ \mathrm{C10}:\ & 0\leq s_{k,l}\leq 1, 0\leq v_l\leq 1,\forall k,l\\ \mathrm{C11}:\ & \sum_{l=1}^L\sum_{k=1}^K s_{k,l}-\sum_{l=1}^L\sum_{k=1}^K s_{k,l}^2\leq 0\\ \mathrm{C12}:\ & \sum_{l=1}^L v_l-\sum_{l=1}^L v_l^2\leq 0\end{aligned} \tag{30}$$

where the constraint (C10) is linear, but the constraints (C11) and (C12) are both difference functions of convex functions. To convexify the constraints (C11) and (C12), we adopt the SCA method, where the concave parts of the constraints (C11) and (C12) can be lower-bounded by their Taylor series expansions. Specifically, using the first-order Taylor series expansion at $\tilde{x}$, x^2 can be lower-bounded by the linear function.

$$g\left(x,\tilde{x}\right)=\tilde{x}^2+2\tilde{x}\left(x-\tilde{x}\right). \tag{31}$$

Thus, one has

$$\sum_{l=1}^L\sum_{k=1}^K s_{k,l}-\sum_{l=1}^L\sum_{k=1}^K s_{k,l}^2\leq\sum_{l=1}^L\sum_{k=1}^K s_{k,l}-\sum_{l=1}^L\sum_{k=1}^K g\left(s_{k,l},\tilde{s}_{k,l}\right), \tag{32}$$

and

$$\sum_{l=1}^L v_l-\sum_{l=1}^L v_l^2\leq\sum_{l=1}^L v_l-\sum_{l=1}^L g\left(v_l,\tilde{v}_l\right), \tag{33}$$

where $\{\tilde{s}_{k,l}\}$ $\{\tilde{v}_l\}$ are Taylor-expansion constants and $g(\cdot,\cdot)$ is given by (31). By approximating the non-convex constraints with linear functions in (32) and (33), the problem (P1.5) can be solved iteratively. The problem during each iteration is given by

$$\begin{aligned}(\mathrm{P1.6})\quad \max_{\substack{\{\mathbf{B}_k\},\mathbf{C},\\ \{s_{k,l}\},\{c_l\}}}\ & |\alpha_0|^2\mathrm{tr}\left(\mathbf{R}_0\mathbf{C}\right)-\tau\sum_{i=1}^I|\alpha_i|^2\mathrm{tr}\left(\mathbf{R}_i\mathbf{C}\right)-\tau\sigma_0^2\\ \text{s.t.}\ & \mathrm{C1}\sim\mathrm{C5},\mathrm{C8},\mathrm{C9}\\ \mathrm{C10}:\ & 0\leq s_{k,l}\leq 1, 0\leq v_l\leq 1,\forall k,l\\ \mathrm{C13}:\ & \sum_{l=1}^L\sum_{k=1}^K s_{k,l}-\sum_{l=1}^L\sum_{k=1}^K g\left(s_{k,l},\tilde{s}_{k,l}\right)\leq 0\\ \mathrm{C14}:\ & \sum_{l=1}^L v_l-\sum_{l=1}^L g\left(v_l,\tilde{v}_l\right)\leq 0\end{aligned} \tag{34}$$

where the constraints (C13) and (C14) are linear constraints. Thus, the problem (P1.6) is a SDP problem, which can be solved using a generic SDP solver.

A sub-optimal solution to the problem (P1.5) can be obtained by solving the problem (P1.6) iteratively. The Taylor-expansion constants $\{\tilde{s}_{k,l}\}$ $\{\tilde{v}_l\}$ are updated by the solution to the problem (P1.6). The convergence can be guaranteed, because the objective function of the problem (P1.6) is upper-bounded and non-decreasing in each iteration .

3) Algorithm of radar-centric design: Combing the above steps, the algorithm to solve the radar-centric problem (P1) in (17) can be summarized in Algorithm 1. The initial point of the iteration can be provided by the following feasible problem, i.e.,

$$
\begin{aligned}
(\text{P1.7}) \quad \max_{\substack{\{\mathbf{B}_k\},\mathbf{C},\\ \{s_{k,l}\},\{c_l\}}} \quad & \sum_{k=1}^{K}\sum_{l=1}^{L} s_{k,l}\beta_{k,l} + \sum_{l=1}^{L} v_l {\beta_l}' \\
\text{s.t.} \quad & \frac{\mathrm{tr}\left(\mathbf{H}_k\mathbf{B}_k\right)}{\mathrm{tr}\left(\mathbf{H}_k\mathbf{C}\right) - \mathrm{tr}\left(\mathbf{H}_k\mathbf{B}_k\right) + \sigma_k^2} \geq \Gamma_k, \forall k \\
& \mathrm{tr}\left(\mathbf{J}_l\mathbf{C}\right) \leq P_l, \forall l \\
& \mathbf{C} \succeq 0, \mathbf{B}_k \succeq 0, \forall k \\
& \mathbf{C} - \sum_{k=1}^{K} \mathbf{B}_k \succeq 0 \\
& 0 \leq s_{k,l} \leq 1, 0 \leq v_l \leq 1, \forall k, l \\
& \mathrm{tr}\left(\mathbf{J}_l\mathbf{B}_k\right) \leq s_{k,l}P_l, \forall k, l \\
& \mathrm{tr}\left[\mathbf{J}_l\left(\mathbf{C} - \sum_{k=1}^{K}\mathbf{B}_k\right)\right] \leq v_l P_l, \forall l
\end{aligned}
\tag{35}
$$

where the backhaul cost is minimized subject to the communication performance constraint. Because l_1-norm relaxation of the clustering variables is adopted, the problem (P1.7) is convex.

Remark 1. (Complexity of Algorithm 1) The complexity to solve the problem (P1.6) is $\mathcal{O}((NL)^{7/2}\log(1/\varepsilon))$ for ε-tolerance in the solution of the interior-point method. Thus, the complexity of Algorithm 1 can be given by $\mathcal{O}((NL)^{7/2}\log(1/\varepsilon_1))\log(1/\varepsilon_2))$.

B. Communication-centric Problem

Compared to the radar-centric problem (P1), the communication-centric problem (P2) in (18) is more complex. Besides the rank-one constraint (C6) of the beamforming vector and the non-continuous clustering variables of both communication and radar, the max-min objective function is a multi-ratio fractional function.

1) Waveform optimization: Similar to the radar-centric problem, we also first consider the communication-centric problem with fixed clustering. After relaxing the constraints (C3) and (C7) on the clustering variables, the original problem (P2) can be simplified to a waveform optimization problem, i.e.,

Algorithm 1 Algorithm of radar-centric waveform and clustering design

1: Initialize the convergence precision ε_1 and ε_2;
2: Solve the feasible problem (P1.7) and obtain the initial clustering variables $s_{k,l}^*$, v_l^* and the initial waveform matrix $\{\mathbf{B}_k^*\}, \mathbf{C}^*$;
3: Compute the initial SINR for the target sensing γ_0^* according to (15);
4: Calculate τ^* based on the initial waveform matrix $\mathbf{C}^*$ according to (21)
5: **repeat**
6: Set $\tau = \tau^*$
7: **repeat**
8: Set $\tilde{s}_{k,l} = s_{k,l}^*$, $\tilde{v}_l = s_l^*$, $\forall k, l$, and $\gamma_0 = \gamma_0^*$
9: Solve the problem (P1.6) given $g\left(s_{k,l}, \tilde{s}_{k,l}\right)$ and $g\left(v_l, \tilde{v}_l\right)$ according to (31) and obtain the optimal $\{\mathbf{B}_k^*\}, \mathbf{C}^*, \{s_{k,l}^*\}, \{c_l^*\}$;
10: Calculate the received SINR for the target sensing γ_0^* according to (15);
11: **until** $|\gamma_0^* - \gamma_0| \leq \varepsilon_1$
12: Calculate τ^* based on $\mathbf{C}^*$ according to (21);
13: **until** $|\tau^* - \tau| \leq \varepsilon_2$
14: **if** $\mathrm{rank}\left(\mathbf{B}_k^*\right) \neq 1$
15: Update $\mathbf{B}_k^*$ according to (23).
16: **end if**

$$
\begin{aligned}
(\text{P2.1}) \quad \max_{\{\mathbf{B}_k\},\mathbf{C}} \min_k \quad & \frac{\mathrm{tr}\left(\mathbf{H}_k\mathbf{B}_k\right)}{\mathrm{tr}\left(\mathbf{H}_k\mathbf{C}\right) - \mathrm{tr}\left(\mathbf{H}_k\mathbf{B}_k\right) + \sigma_k^2} \\
\text{s.t.} \quad & \text{C0, C2, C4} \sim \text{C6, C8, C9}
\end{aligned},
\tag{36}
$$

which optimizes the beamforming vector of the communication signal and the covariance matrix of the dedicated probing signal.

Note that the relaxed problem (P2.1) is also non-convex due to both the objective function and the rank-one constraint (C6). To avoid the multi-ratio fractional function, quadratic transform can be introduced, where the problem (P2.1) can be converted to

$$
\begin{aligned}
(\text{P2.2}) \quad \max_{\{\mathbf{B}_k\},\mathbf{C},\tau} \quad & \tau \\
\text{s.t.} \quad & \text{C0, C2, C4} \sim \text{C6, C8, C9} \\
& q\left(\kappa_k, \mathbf{B}_k, \mathbf{C},\right) \geq \tau, \forall k
\end{aligned},
\tag{37}
$$

where τ, $\{\kappa_k\}$ are the auxiliary variables and

$$
\begin{aligned}
q\left(\kappa_k, \mathbf{B}_k, \mathbf{C},\right) = 2\kappa_k\sqrt{\mathrm{tr}\left(\mathbf{H}_k\mathbf{B}_k\right)} - \kappa_k^2\mathrm{tr}\left(\mathbf{H}_k\mathbf{C}\right) \\
+ \kappa_k^2\mathrm{tr}\left(\mathbf{H}_k\mathbf{B}_k\right) - \kappa_k^2\sigma_k^2
\end{aligned}.
\tag{38}
$$

Then, we have the following lemma on the optimality of the quadratic transform.

Lemma 3. (Optimality of quadratic transform) By alternatively optimizing the problem (P1.2) with fixed $\{\kappa_k\}$ and updating the auxiliary variables $\{\kappa_k\}$ as

$$\kappa_k = \frac{\sqrt{\mathrm{tr}\left(\mathbf{H}_k\mathbf{B}_k\right)}}{\mathrm{tr}\left(\mathbf{H}_k\mathbf{C}\right) - \mathrm{tr}\left(\mathbf{H}_k\mathbf{B}_k\right) + \sigma_k^2}, \forall k, \tag{39}$$

the optimal solution to the problem (P2.2) converges to the global optimal solution to the problem (P2.1).

Proof. According to [50, Corollary 3], the problem (P2.1) is equivalent to the following problem (P2.2)

$$\begin{aligned} (\text{P2.3}) \quad \max_{\{\mathbf{B}_k\},\mathbf{C},\tau,\{\kappa_k\}} \quad & \tau \\ \text{s.t.} \quad & \text{C0, C2, C4} \sim \text{C6, C8, C9} \\ & q\left(\kappa_k, \mathbf{B}_k, \mathbf{C},\right) \geq \tau, \forall k \end{aligned}, \tag{40}$$

To solve the problem (P2.3), $\{\kappa_k\}$ and the other variables can be updated iteratively. Because the problem (P2.1) is a max-min-ratio concave-convex fractional problem, the solution to the problem (P2.2) convergences to the globally optimal solution to the problem (P2.3) by updating $\{\kappa_k\}$ according to (39) iteratively [50, Theorem 4]. It completes the proof. □

The problem (P2.2) is still non-convex due the rank-one constraint (C6). Thus, SDR can be also adopted for the problem (P2.2) and the relaxed problem is given by

$$\begin{aligned} (\text{P2.4}) \quad \max_{\{\mathbf{B}_k\},\mathbf{C},\tau} \quad & \tau \\ \text{s.t.} \quad & \text{C0, C2, C4, C5, C8, C9} \\ & q\left(\kappa_k, \mathbf{B}_k, \mathbf{C},\right) \geq \tau, \forall k \end{aligned}, \tag{41}$$

which is convex with fixed $\{\kappa_k\}$. We can also prove the tightness after SDR according to the following lemma.

Lemma 4. (**Tightness of SDR**) After SDR of the problem (P2.2), the problem (P2.4) is convex and the corresponding global optimal solution can be denoted by $\hat{\mathbf{C}}, \{\tilde{\mathbf{B}}_k\}$. Although $\{\tilde{\mathbf{B}}_k\}$ may not satisfy rank-one constraint, we can obtain a rank-one optimal solution for the problem (P2.4) based on $\{\tilde{\mathbf{B}}_k\}$. That is

$$\hat{\mathbf{B}}_k = \frac{\tilde{\mathbf{B}}_k\mathbf{h}_k\mathbf{h}_k^H\tilde{\mathbf{B}}_k^H}{\mathbf{h}_k^H\tilde{\mathbf{B}}_k\mathbf{h}_k}, \forall k \tag{42}$$

satisfying $\mathrm{rank}(\hat{\mathbf{B}}_k) = 1, \forall k$.

Proof. The proof is similar to that of Lemma 2, which is omitted for the conciseness. □

Also, the waveform optimization problem with fixed clustering, i.e., the problem (P2.1), can be solved according to the following proposition.

Proposition 2. (Solution to waveform optimization) With fixed clustering, the waveform optimization problem (P2.1) can be solved by optimizing the convex SDR problem (P2.4) and updating the auxiliary variable according to (39).

Proof. According to Lemma 4, we can always obtain a rank-one optimal solution after SDR for the problem (P2.4), which is also the optimal solution to the problem (P2.2). Further, according to Lemma 3, the optimal solution to the problem (P2.2) converges to the global optimal solution of the problem (P2.1) by alternatively updating $\{\kappa_k\}$ according to (39). It completes the proof. □

2) Clustering optimization: In the next step, we consider the radar-centric problem with dynamic clustering. Then, the waveform design problem (P2.4) can be reformulated with the constraints (C3) and (C7) considered, i.e.,

$$\begin{aligned} (\text{P2.5}) \quad \max_{\{\mathbf{B}_k\},\mathbf{C},\tau,\{s_{k,l}\},\{c_l\}} \quad & \tau \\ \text{s.t.} \quad & \text{C0, C2} \sim \text{C5, C7} \sim \text{C9} \\ & q\left(\kappa_k, \mathbf{B}_k, \mathbf{C},\right) \geq \tau, \forall k \end{aligned} \tag{43}$$

which is also non-convex due to the clustering variables, i.e., the constraint (C7).

Using the equivalent continuous functions to express the non-continuous clustering variables in (26-29), the problem (2.5) is equivalent to

$$\begin{aligned} (\text{P2.6}) \quad \max_{\{\mathbf{B}_k\},\mathbf{C},\tau,\{s_{k,l}\},\{c_l\}} \quad & \tau \\ \text{s.t.} \quad & \text{C0, C2} \sim \text{C5, C8, C9} \\ & q\left(\kappa_k, \mathbf{B}_k, \mathbf{C},\right) \geq \tau, \forall k \\ \text{C10}: \quad & 0 \leq s_{k,l} \leq 1, 0 \leq v_l \leq 1, \forall k, l \\ \text{C11}: \quad & \sum_{l=1}^{L}\sum_{k=1}^{K} s_{k,l} - \sum_{l=1}^{L}\sum_{k=1}^{K} s_{k,l}^2 \leq 0 \\ \text{C12}: \quad & \sum_{l=1}^{L} v_l - \sum_{l=1}^{L} v_l^2 \leq 0 \end{aligned}, \tag{44}$$

where the non-convex constraints (C11) and (C12) are difference functions of convex functions. SCA can be also adopted to convexify the constraints by their Taylor series expansions. Specifically, the problem (P2.6) can be solved iteratively, and the problem during each iteration can be given by

$$\begin{aligned} (\text{P2.7}) \quad \max_{\substack{\{\mathbf{B}_k\},\mathbf{C},\tau \\ \{s_{k,l}\},\{c_l\}}} \quad & \tau \\ \text{s.t.} \quad & \text{C0, C2} \sim \text{C5, C8, C9} \\ & q\left(\kappa_k, \mathbf{B}_k, \mathbf{C},\right) \geq \tau, \forall k \\ \text{C10}: \quad & 0 \leq s_{k,l} \leq 1, 0 \leq v_l \leq 1, \forall k, l \\ \text{C13}: \quad & \sum_{l=1}^{L}\sum_{k=1}^{K} s_{k,l} - \sum_{l=1}^{L}\sum_{k=1}^{K} g\left(s_{k,l}, \tilde{s}_{k,l}\right) \leq 0 \\ \text{C14}: \quad & \sum_{l=1}^{L} v_l - \sum_{l=1}^{L} g\left(v_l, \tilde{v}_l\right) \leq 0 \end{aligned}, \tag{45}$$

where $g(\cdot,\cdot)$ is given by (31). Thus, the constraints (C13) and (C14) are linear functions. And the problem (P2.7) is an SDP problem, which can be solved using a generic SDP solver.

Also, a sub-optimal solution to the problem (P2.6) can be obtained by solving the problem (P2.7) iteratively. The Taylor-expansion constants $\{\tilde{s}_{k,l}\}$ $\{\tilde{v}_l\}$ are updated by the solution to the problem (P2.7). And the convergence can be guaranteed, because the objective function of the problem (P2.7) is upper-bounded and non-decreasing in each iteration .

3) Algorithm of radar-centric design: The algorithm to solve the radar-centric problem (P2) can be summarized in Algorithm 2. The initial point of the iteration can be provided by the following feasible problem, i.e.,

$$
\begin{aligned}
(\text{P2.8}) \quad \max_{\substack{\{\mathbf{B}_k\},\mathbf{C} \\ \{s_{k,l}\},\{c_l\}}} \quad & \sum_{k=1}^{K}\sum_{l=1}^{L} s_{k,l}\beta_{k,l} + \sum_{l=1}^{L} v_l \beta_l{}' \\
\text{s.t.} \quad & \frac{|\alpha_0|^2 \mathrm{tr}\left(\mathbf{R}\left(\theta_0\right)\mathbf{C}\right)}{\sum_{i=1}^{I}|\alpha_i|^2 \mathrm{tr}\left(\mathbf{R}\left(\theta_i\right)\mathbf{C}\right)+\sigma_0^2} \geq \Gamma_0 \\
& \mathrm{tr}\left(\mathbf{J}_l\mathbf{C}\right) \leq P_l, \forall l \\
& \mathbf{C} \succeq 0, \mathbf{B}_k \succeq 0, \forall k \\
& \mathbf{C} - \sum_{k=1}^{K}\mathbf{B}_k \succeq 0 \\
& 0 \leq s_{k,l} \leq 1, 0 \leq v_l \leq 1, \forall k,l \\
& \mathrm{tr}\left(\mathbf{J}_l\mathbf{B}_k\right) \leq s_{k,l}P_l, \forall k,l \\
& \mathrm{tr}\left[\mathbf{J}_l\left(\mathbf{C} - \sum_{k=1}^{K}\mathbf{B}_k\right)\right] \leq v_l P_l, \forall l
\end{aligned}
\tag{46}
$$

where l_1-norm relaxation of the clustering variables is adopted and the backhaul cost is minimized subject to the radar performance constraint. Thus, the feasible problem (P2.8) is also convex.

Remark 2. (Complexity of Algorithm 2) The complexity to solve the problem (P2.7) is $\mathcal{O}((NL)^{7/2}\log(1/\varepsilon))$ for ε-tolerance in the solution of the interior-point method. Thus, the complexity of Algorithm 2 is also given by $\mathcal{O}((NL)^{7/2}\log(1/\varepsilon_1))\log(1/\varepsilon_2))$.

Algorithm 2 Algorithm of communication-centric waveform and clustering design

1: Initialize the convergence precision ε_1 and ε_2;
2: Solve the feasible problem (P2.8) and obtain the initial clustering variables $s_{k,l}^*$, v_l^* and the initial waveform matrix $\{\mathbf{B}_k^*\}, \mathbf{C}^*$;
3: Compute the initial SINR of the CUs $\{\gamma_k^*\}$ according to (13);
4: Calculate τ^* as $\tau = \min_k\{q\left(\kappa_k, \mathbf{B}_k, \mathbf{C},\right)\}$ according to $q\left(\kappa_k, \mathbf{B}_k, \mathbf{C},\right)$ in (38) and κ_k in (39).
5: **repeat**
6: Set $\tau = \tau^*$
7: **repeat**
8: Set $\tilde{s}_{k,l} = s_{k,l}^*$, $\tilde{v}_l = s_l^*$, and $\gamma_k = \gamma_k^*$, $\forall k,l$
9: Solve the problem (P2.7) given $g\left(s_{k,l}, \tilde{s}_{k,l}\right)$ and $g\left(v_l, \tilde{v}_l\right)$ according to (31) and obtain the optimal $\{\mathbf{B}_k^*\}, \mathbf{C}^*, \tau^*, \{s_{k,l}^*\}, \{c_l^*\}$;
10: Calculate the received SINR of the CUs γ_k^* according to (13);
11: **until** $|\min\{\gamma_k^*\} - \min\{\gamma_k\}| \leq \varepsilon_1$
12: **until** $|\tau^* - \tau| \leq \varepsilon_2$
13: **if** $\mathrm{rank}\left(\mathbf{B}_k^*\right) \neq 1$
14: Update $\mathbf{B}_k^*$ according to (42).
15: **end if**

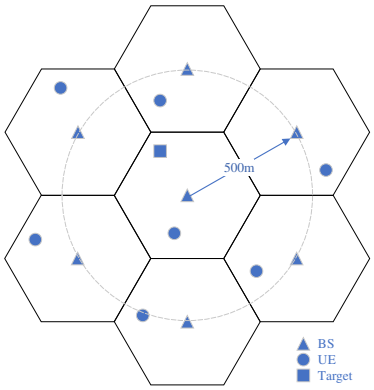

Figure 3. The simulation model of 7 BSs, multiple UEs and a target.

V. Simulation Results and Discussion

In this section, we evaluate the performance of our proposed design for the DFRC system via simulation. The parameter settings are provided as follows unless specified otherwise. We consider a hexagonal multi-cell network as illustrated in Fig. 3, where each BS is located at the center of the cell. The CUs and the target are uniformly and independently distributed in the network, excluding an inner circle of 50m around each BS. The path loss is modeled as PL (dB) $= 148.1 + 37.6\log_{10}(d)$, where d is the distance in kilometers. The small-scale fading is the normalized Rayleigh fading. The parameters are set as Table I unless specified otherwise. All simulation results are obtained using 10^3 Monte-Carlo simulations.

Generally, the target and the clutter will be located at different spatial angles for different BSs. In the simulation, we align the spatial angle of the target to $\theta_0 = 0^\circ$ and the spatial angles of two fixed clutter signals to $\theta_1 = -30^\circ$ and $\theta_2 = 30^\circ$. The maximum backhaul capacity determines the maximum numbers of coordinated BSs. Thus, we adopt different maximum numbers of coordinated BSs L_M to evaluate the impact of backhaul cost.

In Fig. 4, the optimized beampatterns for different maximum numbers of coordinated BSs $L_M = 3, 5, 7$ is shown for radar-centric design. The number of the CU is $K = 6$, and the SINR constraint of the communication is set as $\Gamma_k = 20$ dB. We define the optimized beampattern as $P\left(\theta\right) = |\mathbf{w}^{*H}\mathbf{A}\left(\theta\right)\mathbf{x}|^2$, where $\mathbf{w}^*$ is the optimal receive beamforming vector based on MVDR optimization. The main beam is located at the target's spatial angle $\theta_0 = 0^\circ$, and the nulls are placed at the clutters' spatial angles $\theta_1 = -30^\circ$ and $\theta_2 = 30^\circ$. When the number of the coordinated BSs increases, the performance of beampattern becomes better

Table I
SIMULATION PARAMETERS

Parameter	Value
The number of BSs in the network	$L = 7$
The number of transmit antennas for each BS	$N = 4$
The number of receive antennas for each BS	$M = 4$
The maximum transmit power of each BS	$P_l = 40$W
The maximum transmit power of each BS	$P_l = 40$W
The noise power spectral density	-172 dBm/Hz
The available channel bandwidth	10 MHz
The RCS power to noise ratio of the target	$\alpha_0^2/\sigma_0^2 = -30$ dB
The RCS power to noise ratio of the clutter	$\alpha_i^2/\sigma_0^2 = -10$ dB

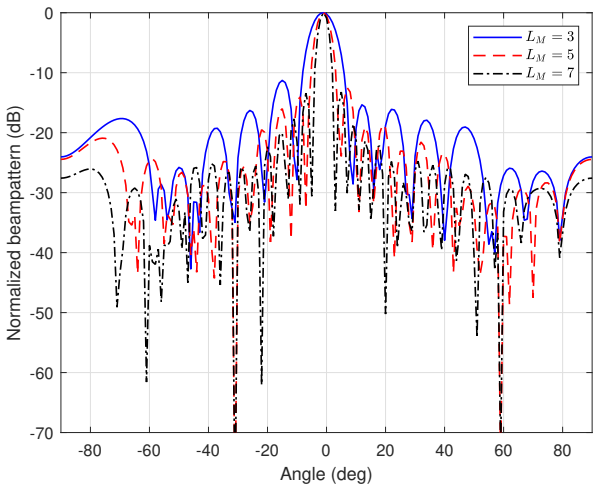

Figure 4. The optimized beampatterns for different maximum numbers of the coordinated BSs ,$L_M = 3, 5, 7$, $K = 6$, $\Gamma_k = 20$ dB.

from the radar's viewpoint. Specifically, the maximum peak to sidelobe ratio decreases with the increase of the number of the coordinated BSs. The beam width of the main lobe also decreases with the increase of the number of the coordinated BSs. The performance gain is at the cost of increased backhaul cost.

The impacts of the communication constraints on the optimized beampatterns are evaluated in Fig. 5 and Fig. 6 with the maximum number of coordinated BSs $L_M = 4$. In Fig. 5, the optimized beammpattern is provided for different numbers of CUs, i.e., $K = 0, 3, 6$, under the SINR constraint $\Gamma_k = 20$ dB. In Fig. 6, the optimized beammpattern is provided for different communication SINR requirements, i.e, $\Gamma_k = 10, 20$ dB with $K = 3$. The radar-only case is provided as a benchmark when $K = 0$, where there is no communication constraint. It provides the best beampatterns from the radar's viewpoint. When the number of the CUs and the SINR constraint of the communication increase, the optimized beampatterns deteriorate. Specifically, the peak-to-sidelobe ratio decreases slightly while the main beam width remains unchanged. This illustrates that the system can still deliver information with an ideal radar beampattern.

We evaluate the convergence performances of the proposed algorithm for different maximum numbers of the coordinated BSs and the CUs in Fig. 7 and Fig. 8, respectively. Based on the proposed Algorithm 1, the received SINR of the

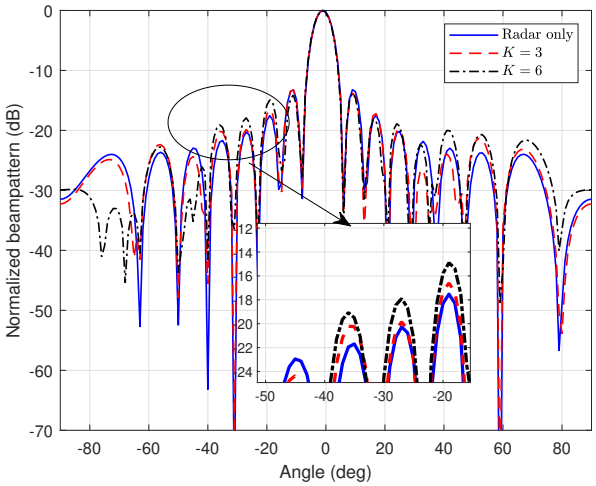

Figure 5. The optimized beampatterns for different numbers of the CUs ,$K = 0, 3, 6$, $L_M = 4$, $\Gamma_k = 20$ dB.

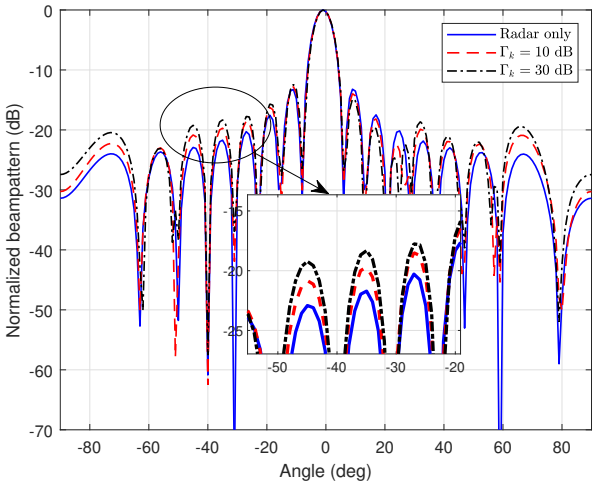

Figure 6. The optimized beampatterns for different SINR constraints of the communication ,$\Gamma_k = 10, 30$ dB, $L_M = 4$, $K = 3$ dB.

radar versus the number of iterations is provided. First, the received SINR of the radar increases during the iteration. This guarantees the convergence of the proposed iterative algorithm. Then, the algorithm requires about 5 iterations to converge for different maximum numbers of the coordinated BSs in Fig. 7. The number of iterations is not affected by the number of the coordinated BSs. The number of iterations increases with the increase of the number of the CUs, as illustrated in Fig. 8. This is because the searching space of the optimization becomes larger when the number of the CUs increases.

In Fig. 9, we compare the proposed clustering scheme with the static clustering scheme with fixed coordinated BSs, and the optimal clustering scheme through exhaustive search. Because the clustering problem belongs to integer programming, which is NP-hard. The optimal clustering has to enumerates all possible candidates for the solution and checking whether each candidate satisfies the problem's statement. The received SINR of the radar is shown for different SINR constraints of

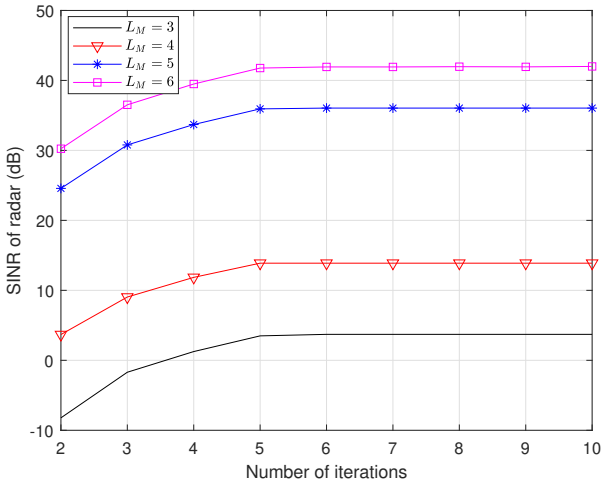

Figure 7. Convergence performance of the proposed radar-centric algorithm for different maximum numbers of the coordinated BSs, $L_M = 3, 4, 5, 6$, $K = 3$, $\Gamma_k = 20$ dB.

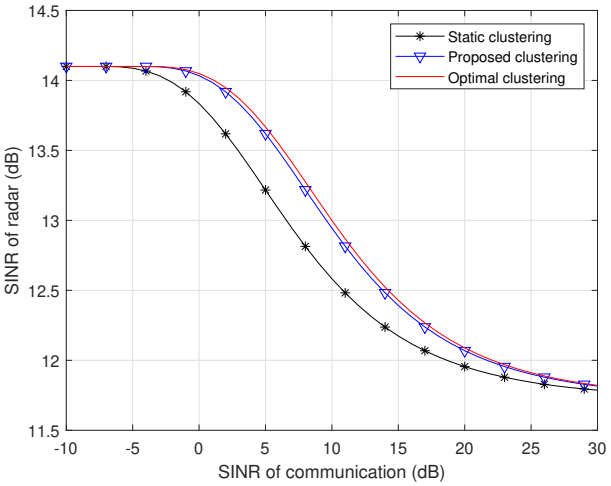

Figure 9. Performance region of the proposed clustering scheme, the static clustering scheme and the optimal clustering scheme, $L_M = 4$, $K = 3$, $\Gamma_k = 20$ dB.

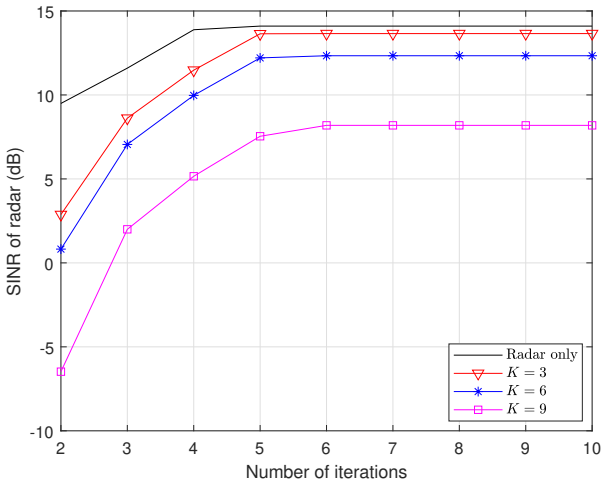

Figure 8. Convergence performance of the proposed radar-centric algorithm for different numbers of the CUs, $K = 0, 3, 6, 9$, $L_M = 4$, $\Gamma_k = 20$ dB.

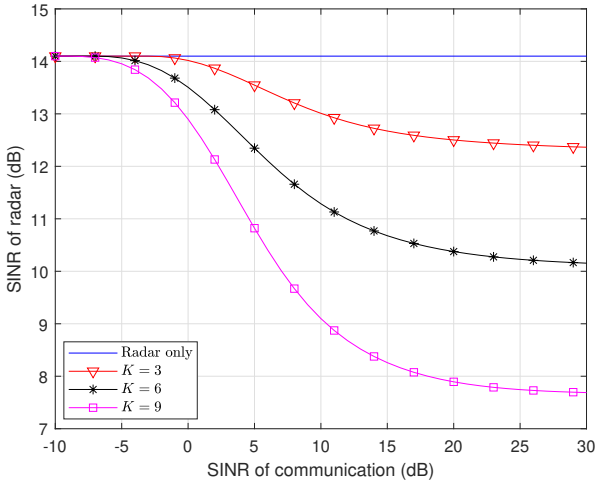

Figure 10. Performance region of the proposed scheme with different numbers of CUs, $K = 0, 3, 6, 9$, $L_M = 4$, $\Gamma_k = 20$ dB.

the communication, where the number of the CUs is $K = 3$ and the maximum number of the coordinated BSs is $L_M = 4$. It actually provides the achievable performance region of the CoMP DFRC system, and the curve depicts the boundary of the region with different clustering schemes. The performance of the proposed clustering scheme is almost the same as that of the exhaustive searching. The slight performance loss is due to the fact that SCA can only provide a sub-optimal solution. Compared with the static clustering scheme, the proposed clustering scheme can achieve a performance gain through the diversity of the coordinated BSs.

The performance region of the coordinated DFRC system is evaluated for the proposed algorithm for different numbers of the CUs in Fig. 10, where the maximum number of the coordinated BSs is $L_M = 4$. First, the received SINR for the radar decreases with the increase of the SINR constraint of the communication. Then, the decreasing rate increases with the increase of the number of CUs. Specifically, the increasing rate of $K = 9$ is much larger than that of $K = 3$. This is because more communication users lead to more communication constraints. Finally, when the SINR constraint of the communication is below -5 dB, the received SINR of the radar is almost unchanged and equals to the radar-only case. This means that the communication constraints have no effect.

VI. Conclusion

In this paper, we have extended the DFRC designs to a CoMP transmission scenario, where communication cluster and radar cluster could be formed to improve the performance of both communication and sensing. We have derived the SINRs of the CUs and the target sensing. Both radar-centric and communication-centric problems have been formulated to optimize the waveform and the clustering for

both communication and radar. We have adopted Dinkelbach's transform and quadratic transform to simplify the fractional objective function for both problems. For the communication beamforming vector with rank-one constraint, SDR has been applied with its tightness proved. Thus, an optimal waveform design has been provided with fixed clustering. When the clustering are dynamic, we have used equivalent continuous functions to express the non-continuous clustering variables of both communication and radar. SCA have been adopted to convexitify the equivalent continuous functions. Thus, a sub-optimal solution has been provided to design the clustering for the CoMP DFRC system. The simulation results have verified the performance gain from the CoMP transmission and the effectiveness of our design.

REFERENCES

[1] A. Moreira, P. Prats-Iraola, M. Younis, G. Krieger, I. Hajnsek, and K. P. Papathanassiou, "A tutorial on synthetic aperture radar," *IEEE Geosci. Remote Sens. Mag.*, vol. 1, no. 1, pp. 6–43, 2013.

[2] C. You and R. Zhang, "3D trajectory optimization in rician fading for uav-enabled data harvesting," *IEEE Trans. Wireless Commun.*, vol. 18, no. 6, pp. 3192–3207, 2019.

[3] Y. He, Y. Chen, Y. Hu, and B. Zeng, "WiFi vision: Sensing, recognition, and detection with commodity MIMO-OFDM wifi," *IEEE Internet Things J.*, vol. 7, no. 9, pp. 8296–8317, 2020.

[4] Y. Cao, S. Xu, J. Liu, and N. Kato, "Toward smart and secure V2X communication in 5G and beyond: A UAV-enabled aerial intelligent reflecting surface solution," *IEEE Veh. Technol. Mag.*, vol. 17, no. 1, pp. 66–73, 2022.

[5] L. Chen, F. Liu, W. Wang, and C. Masouros, "Joint radar-communication transmission: A generalized pareto optimization framework," *IEEE Trans. Signal Process.*, vol. 69, pp. 2752–2765, 2021.

[6] Z. Xiao and Y. Zeng, "Waveform design and performance analysis for full-duplex integrated sensing and communication," *IEEE J. Sel. Areas Commun.*, vol. 40, no. 6, pp. 1823–1837, 2022.

[7] X. Mu, Y. Liu, L. Guo, J. Lin, and L. Hanzo, "NOMA-aided joint radar and multicast-unicast communication systems," *IEEE J. Sel. Areas Commun.*, vol. 40, no. 6, pp. 1978–1992, 2022.

[8] L. Chen, Z. Wang, Y. Du, Y. Chen, and F. R. Yu, "Generalized transceiver beamforming for DFRC with MIMO radar and MU-MIMO communication," *IEEE J. Sel. Areas Commun.*, vol. 40, no. 6, pp. 1795–1808, 2022.

[9] Y. Chen, J. Zhang, W. Feng, and M.-S. Alouini, "Radio sensing using 5G signals: Concepts, state of the art, and challenges," *IEEE Internet Things J.*, vol. 9, no. 2, pp. 1037–1052, 2022.

[10] A. Hassanien, M. G. Amin, Y. D. Zhang, and F. Ahmad, "Dual-function radar-communications: Information embedding using sidelobe control and waveform diversity," *IEEE Trans. Signal Process.*, vol. 64, no. 8, pp. 2168–2181, 2016.

[11] ——, "Phase-modulation based dual-function radar-communications," *IET Radar Sonar Navig.*, vol. 10, no. 8, pp. 1411–1421, 2016.

[12] T. W. Tedesso and R. Romero, "Code shift keying based joint radar and communications for EMCON applications," *Digital Signal Process.*, vol. 80, pp. 48–56, 2018.

[13] A. Hassanien, M. G. Amin, E. Aboutanios, and B. Himed, "Dual-function radar communication systems: A solution to the spectrum congestion problem," *IEEE Signal Process Mag.*, vol. 36, no. 5, pp. 115–126, 2019.

[14] X. Wang, A. Hassanien, and M. G. Amin, "Dual-function MIMO radar communications system design via sparse array optimization," *IEEE Trans. Aerosp. Electron. Syst.*, vol. 55, no. 3, pp. 1213–1226, 2019.

[15] W. Baxter, E. Aboutanios, and A. Hassanien, "Joint radar and communications for frequency-hopped mimo systems," *IEEE Trans. Signal Process.*, vol. 70, pp. 729–742, 2022.

[16] C. Sturm and W. Wiesbeck, "Waveform design and signal processing aspects for fusion of wireless communications and radar sensing," *Proc. IEEE*, vol. 99, no. 7, pp. 1236–1259, 2011.

[17] P. Kumari, S. A. Vorobyov, and R. W. Heath, "Adaptive virtual waveform design for millimeter-wave joint communication–radar," *IEEE Trans. Signal Process.*, vol. 68, pp. 715–730, 2020.

[18] N. Cao, Y. Chen, X. Gu, and W. Feng, "Joint bi-static radar and communications designs for intelligent transportation," *IEEE Trans. Veh. Technol.*, vol. 69, no. 11, pp. 13 060–13 071, 2020.

[19] Q. Zhang, H. Sun, X. Gao, X. Wang, and Z. Feng, "Time-division ISAC enabled connected automated vehicles cooperation algorithm design and performance evaluation," *IEEE J. Sel. Areas Commun.*, vol. 40, no. 7, pp. 2206–2218, 2022.

[20] V. Petrov, G. Fodor, J. Kokkoniemi, D. Moltchanov, J. Lehtomaki, S. Andreev, Y. Koucheryavy, M. Juntti, and M. Valkama, "On unified vehicular communications and radar sensing in millimeter-wave and low terahertz bands," *IEEE Wireless Commun.*, vol. 26, no. 3, pp. 146–153, 2019.

[21] W. Yuan, Z. Wei, S. Li, J. Yuan, and D. W. K. Ng, "Integrated sensing and communication-assisted orthogonal time frequency space transmission for vehicular networks," *IEEE J. Sel. Top. Signal Process.*, vol. 15, no. 6, pp. 1515–1528, 2021.

[22] N. Cao, Y. Chen, X. Gu, and W. Feng, "Joint radar-communication waveform designs using signals from multiplexed users," *IEEE Trans. Commun.*, vol. 68, no. 8, pp. 5216–5227, 2020.

[23] F. Liu, C. Masouros, A. Li, H. Sun, and L. Hanzo, "MU-MIMO communications with MIMO radar: From co-existence to joint transmission," *IEEE Trans. Wirel. Commun.*, vol. 17, no. 4, pp. 2755–2770, 2018.

[24] X. Liu, T. Huang, N. Shlezinger, Y. Liu, J. Zhou, and Y. C. Eldar, "Joint transmit beamforming for multiuser MIMO communications and MIMO radar," *IEEE Trans. Signal Process.*, vol. 68, pp. 3929–3944, 2020.

[25] T. Huang, N. Shlezinger, X. Xu, Y. Liu, and Y. C. Eldar, "MAJoRCom: A dual-function radar communication system using index modulation," *IEEE Trans. Signal Process.*, vol. 68, pp. 3423–3438, 2020.

[26] N. Su, F. Liu, and C. Masouros, "Secure radar-communication systems with malicious targets: Integrating radar, communications and jamming functionalities," *IEEE Trans. Wireless Commun.*, vol. 20, no. 1, pp. 83–95, 2021.

[27] Y. He, Y. Cai, H. Mao, and G. Yu, "Ris-assisted communication radar coexistence: Joint beamforming design and analysis," *IEEE J. Sel. Areas Commun.*, vol. 40, no. 7, pp. 2131–2145, 2022.

[28] R. Liu, M. Li, Y. Liu, Q. Wu, and Q. Liu, "Joint transmit waveform and passive beamforming design for RIS-Aided DFRC systems," *IEEE J. Sel. Top. Signal Process.*, pp. 1–1, 2022.

[29] W. Wu, G. Han, Y. Cao, Y. Huang, and T.-S. Yeo, "MIMO waveform design for dual functions of radar and communication with space-time coding," *IEEE J. Sel. Areas Commun.*, vol. 40, no. 6, pp. 1906–1917, 2022.

[30] X. Liu, T. Huang, and Y. Liu, "Transmit design for joint MIMO radar and multiuser communications with transmit covariance constraint," *IEEE J. Sel. Areas Commun.*, vol. 40, no. 6, pp. 1932–1950, 2022.

[31] Z. Cheng, Z. He, and B. Liao, "Hybrid beamforming design for OFDM dual-function radar-communication system," *IEEE J. Sel. Top. Signal Process.*, vol. 15, no. 6, pp. 1455–1467, 2021.

[32] D. Gesbert, S. Hanly, H. Huang, S. Shamai Shitz, O. Simeone, and W. Yu, "Multi-cell MIMO cooperative networks: A new look at interference," *IEEE J. Sel. Areas Commun.*, vol. 28, no. 9, pp. 1380–1408, 2010.

[33] W. Yu, T. Kwon, and C. Shin, "Multicell coordination via joint scheduling, beamforming, and power spectrum adaptation," *IEEE Trans. Wireless Commun.*, vol. 12, no. 7, pp. 1–14, 2013.

[34] J. Zhao, T. Q. S. Quek, and Z. Lei, "Coordinated multipoint transmission with limited backhaul data transfer," *IEEE Trans. Wireless Commun.*, vol. 12, no. 6, pp. 2762–2775, 2013.

[35] L. Liu, S. Zhang, and R. Zhang, "Comp in the sky: UAV placement and movement optimization for multi-user communications," *IEEE Trans. Commun.*, vol. 67, no. 8, pp. 5645–5658, 2019.

[36] D. W. K. Ng and R. Schober, "Secure and green SWIPT in distributed antenna networks with limited backhaul capacity," *IEEE Trans. Wireless Commun.*, vol. 14, no. 9, pp. 5082–5097, 2015.

[37] X. Peng, Y. Shi, J. Zhang, and K. B. Letaief, "Layered group sparse beamforming for cache-enabled green wireless networks," *IEEE Trans. Commun.*, vol. 65, no. 12, pp. 5589–5603, 2017.

[38] A. M. Haimovich, R. S. Blum, and L. J. Cimini, "MIMO radar with widely separated antennas," *IEEE Signal Process Mag.*, vol. 25, no. 1, pp. 116–129, 2008.

[39] H. Godrich, A. M. Haimovich, and R. S. Blum, "Target localization accuracy gain in MIMO radar-based systems," *IEEE Trans. Inf. Theory*, vol. 56, no. 6, pp. 2783–2803, 2010.

[40] P. Wang and H. Li, "Target detection with imperfect waveform separation in distributed MIMO radar," *IEEE Trans. Signal Process.*, vol. 68, pp. 793–807, 2020.

[41] H. Song, G. Wen, Y. Liang, L. Zhu, and D. Luo, "Target localization and clock refinement in distributed MIMO radar systems with time synchronization errors," *IEEE Trans. Signal Process.*, vol. 69, pp. 3088–3103, 2021.
[42] A. Zhang, M. L. Rahman, X. Huang, Y. J. Guo, S. Chen, and R. W. Heath, "Perceptive mobile networks: Cellular networks with radio vision via joint communication and radar sensing," *IEEE Veh. Technol. Mag.*, vol. 16, no. 2, pp. 20–30, 2021.
[43] X. Wang, Z. Fei, J. A. Zhang, J. Huang, and J. Yuan, "Constrained utility maximization in dual-functional radar-communication Multi-UAV networks," *IEEE Trans. Commun.*, vol. 69, no. 4, pp. 2660–2672, 2021.
[44] Y. Huang, Y. Fang, X. Li, and J. Xu, "Coordinated power control for network integrated sensing and communication," *arXiv preprint arXiv:2203.09032*, 2022.
[45] S. Gezici, Z. Tian, G. B. Giannakis, H. Kobayashi, A. F. Molisch, H. V. Poor, and Z. Sahinoglu, "Localization via ultra-wideband radios: a look at positioning aspects for future sensor networks," *IEEE Signal Process Mag.*, vol. 22, no. 4, pp. 70–84, 2005.
[46] J. Capon, "High-resolution frequency-wavenumber spectrum analysis," *Proc. IEEE*, vol. 57, no. 8, pp. 1408–1418, 1969.
[47] Eduard, Jorswieck, Alessio, and Zappone, "Energy efficiency in wireless networks via fractional programming theory," *Foundations Trends Commun. Inf. Theory*, 2014.
[48] Z. Luo, W. Ma, A. M. So, Y. Ye, and S. Zhang, "Semidefinite relaxation of quadratic optimization problems," *IEEE Signal Process Mag.*, vol. 27, no. 3, pp. 20–34, 2010.
[49] E. Che, H. D. Tuan, and H. H. Nguyen, "Joint optimization of cooperative beamforming and relay assignment in multi-user wireless relay networks," *IEEE Trans. Wireless Commun.*, vol. 13, no. 10, pp. 5481–5495, 2014.
[50] K. Shen and W. Yu, "Fractional programming for communication systems—part I: Power control and beamforming," *IEEE Trans. Signal Process.*, vol. 66, no. 10, pp. 2616–2630, 2018.

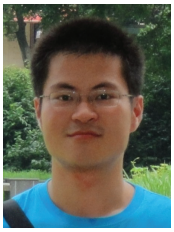

Li Chen received the B.E. in electrical and information engineering from Harbin Institute of Technology, Harbin, China, in 2009 and the Ph.D. degree in electrical engineering from the University of Science and Technology of China, Hefei, China, in 2014. He is currently an Associate Professor with the Department of Electronic Engineering and Information Science, University of Science and Technology of China. His research interests include integrated communication and computation and integrated communication and sensing.

Xiaowei Qin received the B.S. and Ph.D. degrees from the Department of Electrical Engineering and Information Science, University of Science and Technology of China (USTC), Hefei, China, in 2000 and 2008, respectively, where he has been a Member of Staff with the Key Laboratory of Wireless-Optical Communications, Chinese Academy of Sciences, since 2014. His research interests include optimization theory, service modeling in future heterogeneous networks, and wireless artificial intelligence in mobile communication networks.

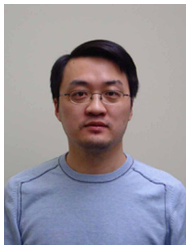

Yunfei Chen (S'02-M'06-SM'10) received his B.E. and M.E. degrees in electronics engineering from Shanghai Jiaotong University, Shanghai, P.R.China, in 1998 and 2001, respectively. He received his Ph.D. degree from the University of Alberta in 2006. He is currently working as a Professor in the Department of Engineering at the University of Durham, UK. His research interests include wireless communications, cognitive radios, wireless relaying and energy harvesting.

Nan Zhao (S'08-M'11-SM'16) is currently a Professor at Dalian University of Technology, China. He received the Ph.D. degree in information and communication engineering in 2011, from Harbin Institute of Technology, Harbin, China.

Dr. Zhao is serving or served on the editorial boards of 7 SCI-indexed journals, including IEEE Transactions on Green Communications and Networking. He won the best paper awards in IEEE VTC 2017 Spring, MLICOM 2017, ICNC 2018, WCSP 2018 and CSPS 2018. He also received the IEEE Communications Society Asia Pacific Board Outstanding Young Researcher Award in 2018.